Lv. 2016. *Int. J. Vehicle Structures & Systems*, 8(3), 161-166
ISSN: 0975-3060 (Print), 0975-3540 (Online)
doi: 10.4273/ijvss.8.3.08

International Journal of Vehicle Structures & Systems
Available online at www.maftree.org/eja

Characteristics and Mechanical Properties of Rolling-Element Bearings

Haiting Lv[a,b]

[a]*School of Mech. Engg., Dalian University of Tech., Dalian, China*
[b]*Dalian Institute of Science Technology, Dalian, China*
Email: Lvhaiting2016@126.com

ABSTRACT:

Large rolling bearings are mainly used in occasions of low speed and heavy load due to its desirable properties such as large-scale structure and high bearing capacity. Currently, the research emphases of large rolling bearings are focussed on the load distribution, load carrying capacity, fatigue life and structure optimization. Bearings used in heavy vehicles belong to large bearings, whose reliability is also very important. In this paper, the characteristics of the structures of four point angular contact ball bearings and three row cylindrical roller bearing are analyzed. Finite element (FE) model is used to simulate the load distribution and angle variation in the actual working process of a large rolling bearing. In order to analyze the impact of the constraints, the stiffness and the local hard point of the supporting structure on the mechanical properties of large rolling bearings, a series of simplified FE models of large rolling bearing with different constraints and supporting structure has been carried out.

KEYWORDS:

Large rolling bearing; Finite element model; Mechanical properties; Contact mechanics

CITATION:

H. Lv. 2016. Characteristics and Mechanical Properties of Rolling-Element Bearings, *Int. J. Vehicle Structures & Systems*, 8(3), 161-166. doi:10.4273/ijvss.8.3.08.

ACRONYMS & NOMENCLATURE:

D_i, D_o	*Inner and outer diameter of bearing*
D_m	*Diameter of distribution circle of roller*
D_w	*Diameter of roller*
r_i, r_o	*Curvature radius of inner and outer bearing ring*
C_{i1}, C_{i2}	*Curvature center of inner ring upward and downward groove*
C_{o1}, C_{o2}	*Curvature center of outer ring upward and downward groove*
D_{w1}	*Diameter of axial bearing roller in upward groove*
D_{w2}	*Diameter of radial bearing roller in middle groove*
D_{w3}	*Diameter of axial bearing roller in downward groove*
a, b	*Major and minor axis of elliptical contact*
β	*Contact angle*

1. Introduction

Bearing is one of the core components of the power generation system and heavy vehicles. Predicting the rolling bearing life plays a crucial role in the reliability and safety of a power plant [1]. Currently, the research emphases of large rolling bearings are focussed on the load distribution, load carrying capacity, fatigue life and structure optimization as well as the application in aeronautics field [2]. Diagnosis and exclusion of the barriers in the system are very important links of the working process [3]-[5]. Mireia [6] established single-row four-point contact bearing and full model with support structure considering deformation of ring and its support structure of bearing. By means of finite element (FE) analysis software, they made more realistic simulation of the bearing load distribution and the contact angle of the bearing. Kania et al [7] established angular contact ball bearings, four point angular contact ball bearing, double row four point contact ball bearing and three row cylindrical roller bearing by using the super element method. By simplified FE model, they have analyzed the mechanical properties of various types of bearings. Kai [8] established Elasto Hydrodynamic Lubrication (EHL) model with the consideration of the spin motion. In order to reduce the starting wind speed decrease of wind turbines, Gang et al [9] studied the design and mechanical properties of permanent magnetic bearings for vertical wind turbines.

In this paper, FE analysis method is used to analyse the large rolling bearing with elasticity support using Hertz contact theory. With this FE model, the load distribution of the roller and angle variation with the actual working process of a large rolling bearing is simulated. In order to analyze the impact of the stiffness and local hard point of the supporting structure on the mechanical properties of large rolling bearings, a series of simplified FE models of large rolling bearing with different constraints and supporting structure has been analysed.

2. Simplified FE models

2.1. Four-point angular contact ball bearing

The geometric structure of four point angular contact ball bearing [10] is shown in Fig. 1(a). The bearing composed of four groove surfaces. The simplified bearing structure by super element method is shown in Fig. 1(b). Each roller is replaced by eight rigid rods and two nonlinear springs. The endpoints of first spring are C_{i1} and C_{o2}. The endpoints of second spring are C_{i2} and C_{o1}. C_{i1} is connected with the inner ring upward groove

through the two rigid rods. C_{i2} is connected with the inner ring downward groove through the two rigid rods. C_{o1} is connected with the outer ring upward groove through the two rigid rods. C_{o2} is connected with the outer ring downward groove through the two rigid rods. Four point angular contact ball bearing deforms under external loading. The contact angle β is the angle between the nonlinear spring and the radial bearing as shown in Fig. 1(c). Simplified FE model of large four-point angular contact ball bearing mainly simulates the compression of roller through the nonlinear springs which connecting the two channel curvature centers. Simplified FE model of large four-point angular contact ball bearing is shown in Fig. 2.

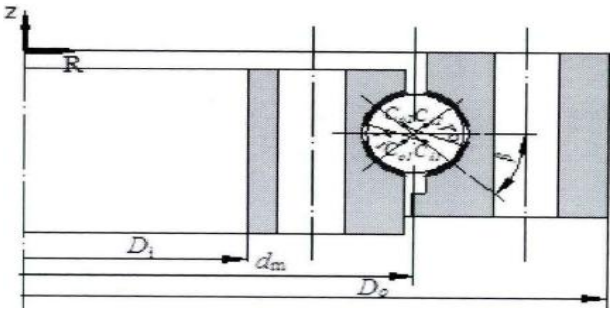

Fig. 1(a): 4-point angular contact ball bearing structure

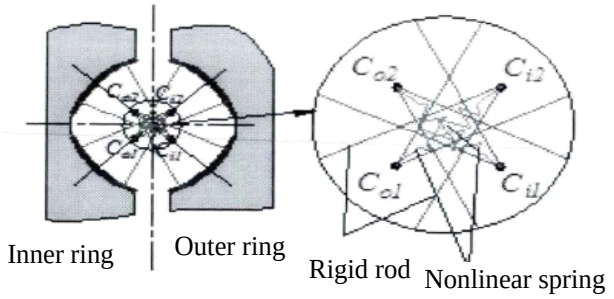

Fig. 1(b): Super element with spring elements and rigid elements

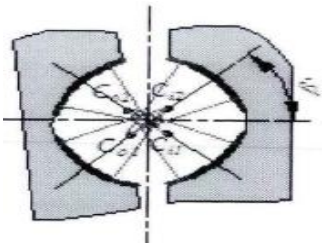

Fig. 1(c): Contact angle β

Fig. 1: Structure & details of 4-point angular contact ball bearing

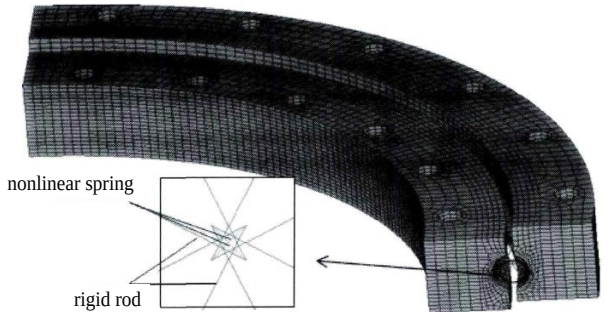

Fig. 2: Simplified FE model of 4-point angular contact ball bearing

2.2. Three row cylindrical roller bearing

The structure of three row cylindrical roller bearing is shown in Fig. 3(a). The bearing rings are composed of two parts which are used to assemble and disassemble the roller. The bearing has three grooves. Three row cylindrical roller bearing can also be classified into cylindrical roller bearings with same diameter and cylindrical roller bearings with different diameters. The simplified roller structure by super element method is shown in Fig. 3(b). Each roller is replaced by a nonlinear spring. One end of the spring is connected with groove surface of outer ring of the bearing. The other end of the spring is connected with groove surface of outer ring of the bearing. As three row cylindrical roller bearing is pressed under external loading, the nonlinear spring works under unidirectional pressure by pulling is used to make the simplification. Simplified FE model of three row cylindrical roller bearing is shown in Fig. 4.

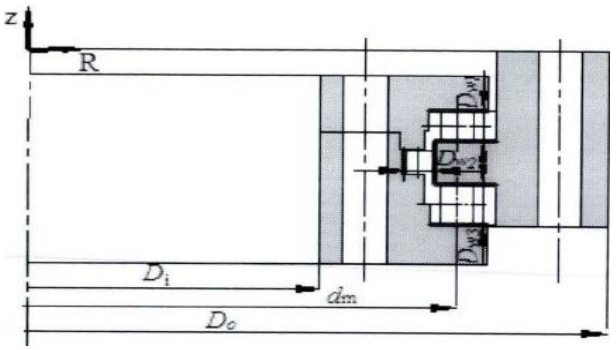

Fig. 3(a): 3- row cylindrical roller bearing structure

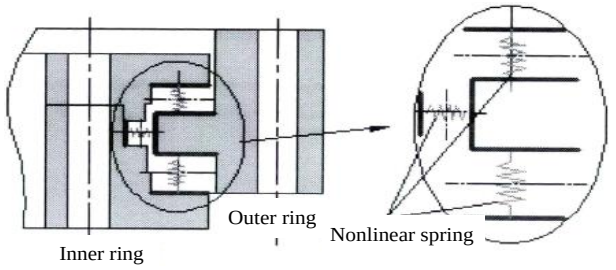

Fig. 3(b): Super element with spring elements and rigid elements

Fig. 3: Structure & details of of 3-row cylindrical roller bearing

Fig. 4: FE model of three row cylindrical roller bearing

2.3. Calculation of non-linear spring stiffness

According to Hertz contact theory, the contact surface and deformation of bearing ball and groove are given by,

$$a = a^* \left[\frac{3Q}{2\sum \rho} \left(\frac{\left(1-\xi_I^2\right)}{E_I} + \frac{1-\xi_{II}^2}{E_{II}} \right) \right]^{\frac{1}{3}} \quad (1)$$

$$b = b^*\left[\frac{3Q}{2\sum\rho}\left(\frac{\left(1-\xi_I^2\right)}{E_I}+\frac{1-\xi_{II}^2}{E_{II}}\right)\right]^{\frac{1}{3}} \tag{2}$$

$$\delta = \delta^*\left[\frac{3Q}{2\sum\rho}\left(\frac{\left(1-\xi_I^2\right)}{E_I}+\frac{1-\xi_{II}^2}{E_{II}}\right)\right]^{\frac{2}{3}}\frac{\sum\rho}{2} \tag{3}$$

Where *a* and *b* are the semi major and minor axes of the contact ellipse and δ is the relative elastic deformation. For the elliptic contact area, the maximum contact stress appears in the geometric center of the ellipse. The normal stress of other points in contact area is given by,

$$\sigma = \frac{3Q}{2\pi ab}\left[1-\left(\frac{x}{a}\right)^2-\left(\frac{y}{b}\right)^2\right] \tag{4}$$

The deformation δ of the spring includes two parts namely, δ_i of roller contacting the inner ring of the bearing and δ_o of roller contacting the outer ring of the bearing as follows,

$$\delta = \delta_i + \delta_o \tag{5}$$

$$\delta = \left\{\begin{array}{l}\delta_i^*\left[\frac{3}{2\sum\rho_i}\left(\frac{\left(1-\xi_{II}^2\right)}{E_{II}}+\frac{\left(1-\xi_{III}^2\right)}{E_{III}}\right)\right]^{\frac{2}{3}}\frac{\sum\rho_i}{2}+\\ \delta_o^*\left[\frac{3}{2\sum\rho_o}\left(\frac{\left(1-\xi_{oI}^2\right)}{E_{oI}}+\frac{\left(1-\xi_{oII}^2\right)}{E_{oII}}\right)\right]^{\frac{2}{3}}\frac{\sum\rho_o}{2}\end{array}\right\}Q^{\frac{2}{3}} \tag{6}$$

3. Effect of support structure constraints and stiffness on mechanical properties

3.1. Effect of supporting structure constraint

The way of supporting the large rolling bearing has a certain effect on the load distribution of the roller inside the bearing. Models of three different supporting structures as shown in Fig. 5 are established. Fig. 5(a) is the whole hub model including blade root housing, bearing and reinforcing plate. Restricted region is the connecting surface of hub and main spindle. Fig. 5(b) is part of hub model including the blade root housing, bearing and reinforcing plate. Restricted region is the lower face of the hub body. Fig. 5(c) is a rigid outer ring model with only the bearing. The restricted region is the outer surface of the outer ring of the bearing. The load of the whole hub model and part hub model is applied on the upper portion of blade root housing. The rigid load of outer ring is applied on the upper end of inner ring of the bearing. Figs. 7 and 8 show the load distribution of first and second groove of the three models. Figs. 9 and 10 show the contact angle of first and second groove of three supporting models simulation.

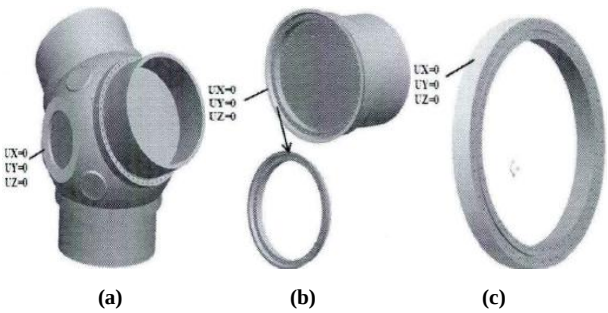

Fig. 5: Three supporting structures of the bearing

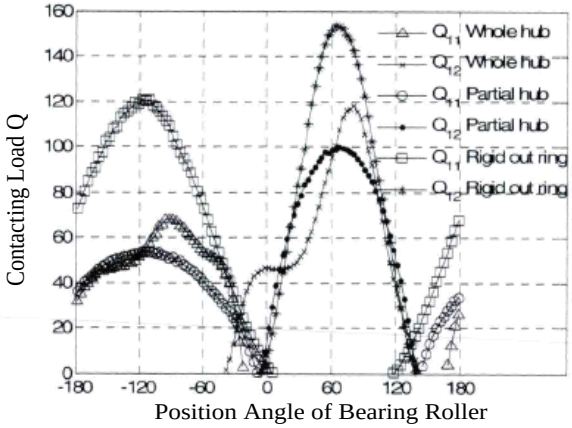

Fig. 6: Contacting load of the roller in first groove

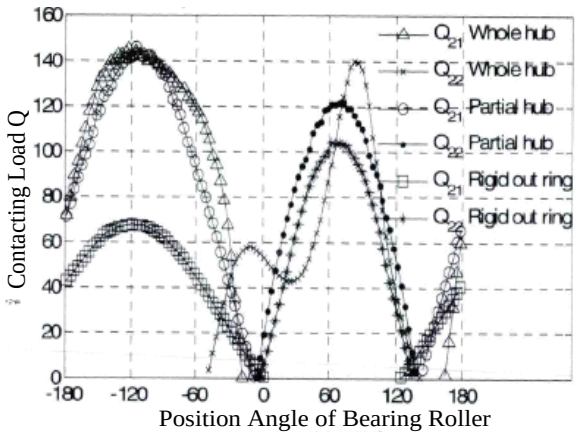

Fig. 7: Contacting load of the roller in second groove

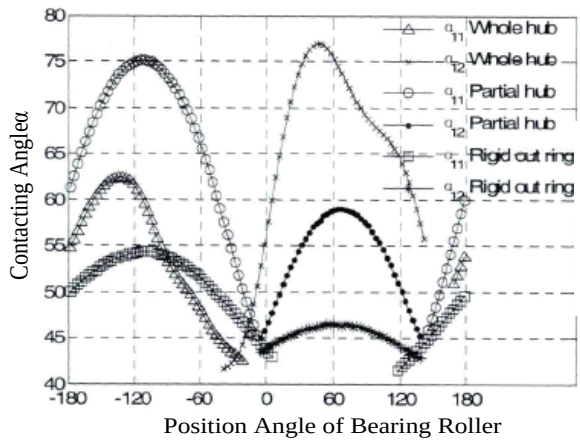

Fig. 8: Connecting angle of rollers in first groove

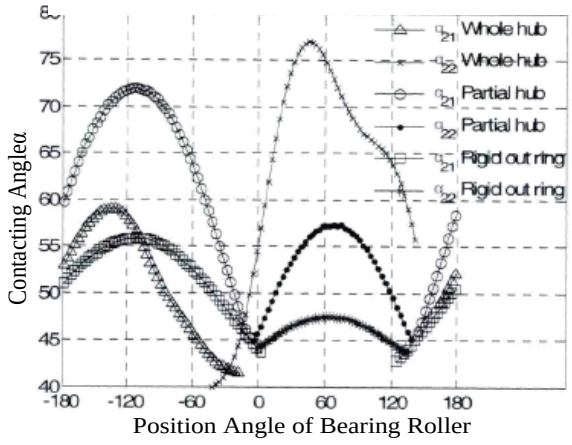

Fig. 9: Connecting angle of rollers in second groove

3.2. Influence of support structure local stiffness

In order to analyze the influence of local stiffness of the support structure on the mechanical properties of bearing, part hub models have been used. Four bearing supporting models with the heights of part hub as 450mm, 650mm, 850mm and 1050mm as shown in Fig. 10 are developed. Lower section of the hub is selected as the constrained surface of the model. When the height of part hub gradually increases, the stiffness of support structure of the bearing reduces. The stiffness of support surface distributes the load circumferentially more unevenly as influenced by hub hole and the changes of wall thickness. By analysis of the loading results as presented in Figs. 11 and 12, it can be known that when the height of part hub is 450mm and 650mm, the load on the roller is close to a cosine distribution. When the hub height is 850mm and 1050mm, loads on the roller Q_{11} and Q_{22} show obvious fluctuations. From distribution shape of roller contact angle as shown in Figs. 13 and 14, it can be established that the contact angle approximates to a cosine distribution. The distribution is smooth and is not affected by local stiff points of the support structure of the bearings.

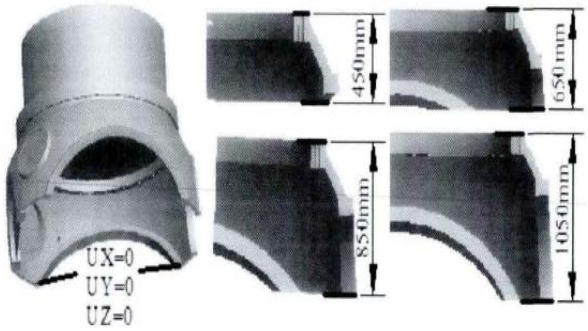

Fig. 10: Part hub models with different supporting heights

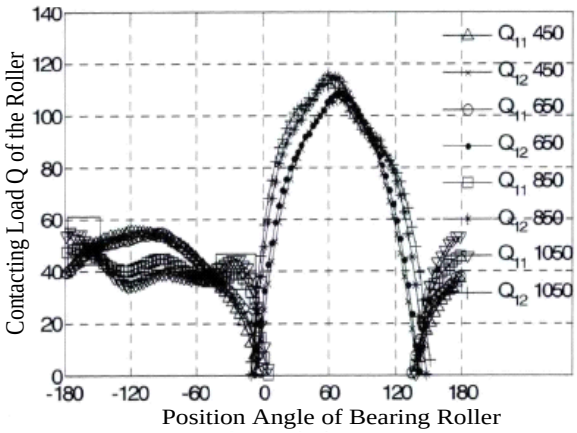

Fig. 11: Contacting loads of rollers in first groove

3.3. Influence of support structure whole stiffness

In order to analyze the influence of whole stiffness of supporting structure on mechanical properties of bearing, whole hub model is established. The hub thickness increases gradually from 65mm increased to 185mm with the increasing interval of 30 mm. In this way, four bearing supporting models with different heights of hubs can be established as shown in Fig. 15. The constriction surface of the model is still r assembling face of the hub and main spindle.

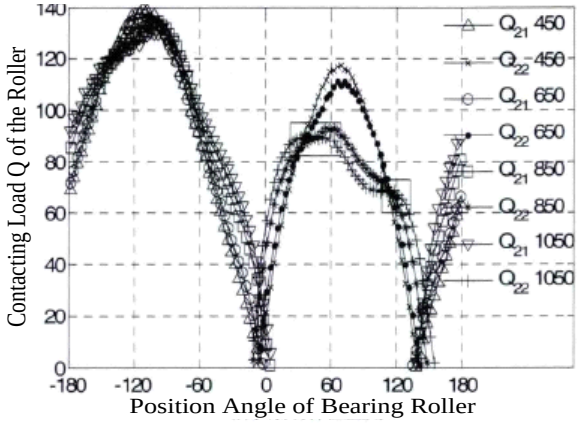

Fig. 12: Contacting loads of rollers in second groove

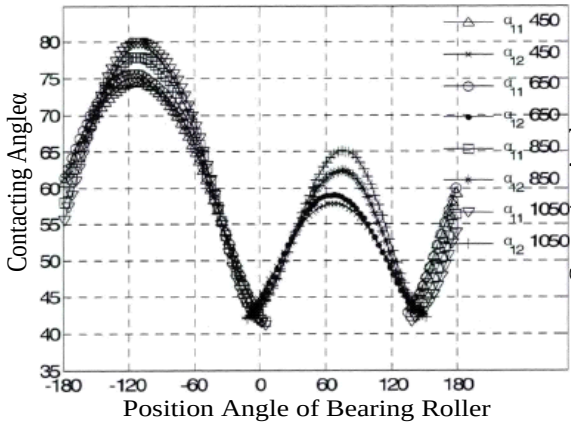

Fig. 13: Connecting angle of rollers in first groove

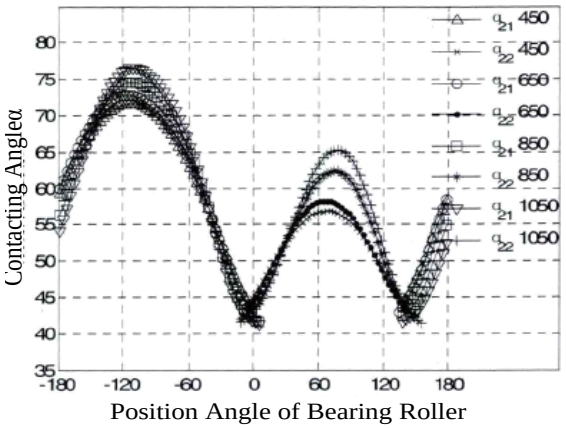

Fig. 14: Connecting angle of rollers in second groove

Through analyzing Figs. 16 and 17, it can be shown that when flexible support stiffness of bearing increases gradually, its influence the on load distribution of bearing roller becomes smaller and smaller. When flexible support stiffness increases to a certain degree, the load distribution of bearing roller generally remains unchanged. By the analysis of the contacting angles as shown in Figs. 18 and 19, it can be shown that when the hub thickness gradually increases, the contacting angle of the roller gradually decreases, which indicates that when the stiffness of bearing support structure increases, the deformation of the bearing decreases and contacting angle of the roller also decreases.

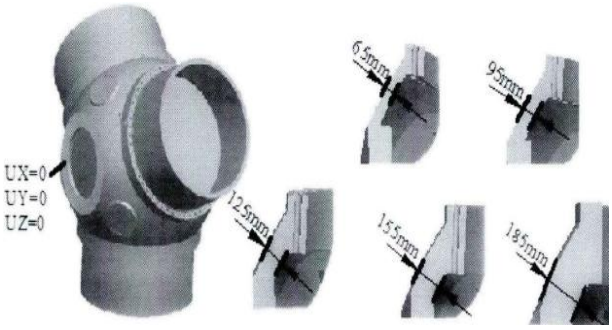

Fig. 15: Different thicknesses of the hub

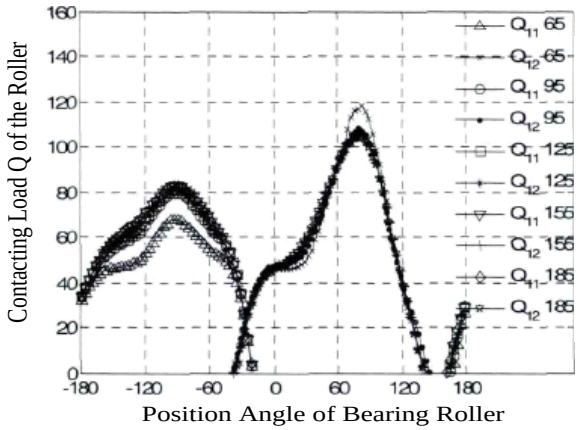

Fig. 16: Contacting loads of rollers in first groove

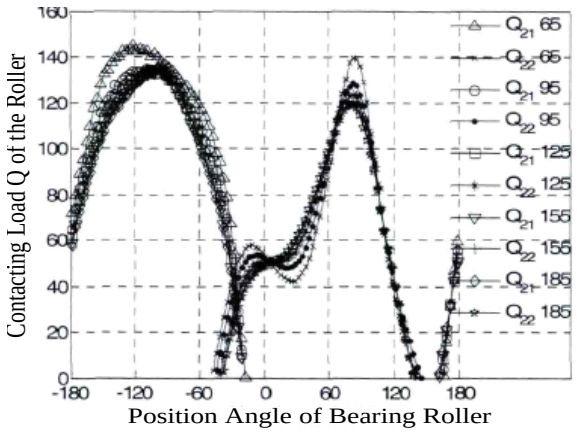

Fig. 17: Contacting loads of rollers in second groove

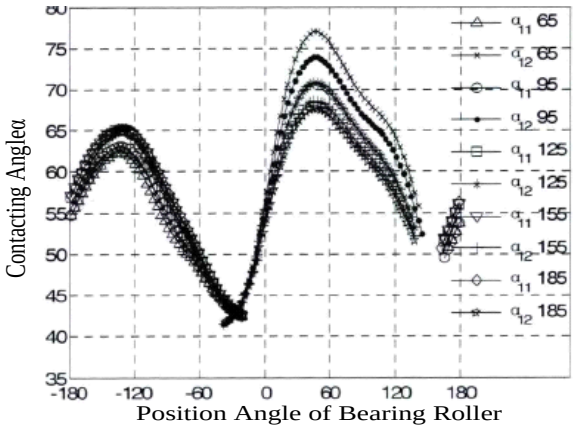

Fig. 18: Contacting angle of rollers in first groove

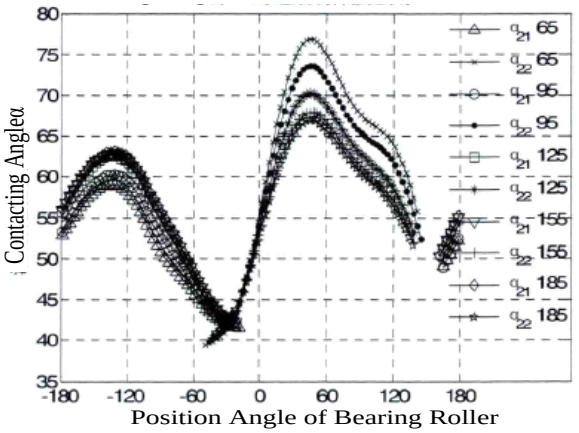

Fig. 19: Contacting angle of rollers in second groove

4. Conclusion

According to the characteristics and mechanical properties of large rolling bearings, this paper proposed a simplified FE model of large rolling bearing and a detailed analysis of the model was carried out. Complex supporting structure of the bearing has increased the local stiffness of supporting surface of large rolling bearing and result in the localised stresses due to stiff points on the contact. When the stiffness of support structure reduces, loads in the two grooves of the bearing tend to be uniform, and maximum load of bearing in each groove has reduced. However, the contacting angle of bearing roller has increased. At this time, the contacting area of roller and groove has reached beyond the edge of the groove. Whole stiffness of the support structure should not be too low as this will increase the contacting angle and reduce the load carrying capacity of the bearing. The stiffness of supporting structure should not be too high as this will lead load distribution to be concentrated in a few rollers, increasing the maximum load on the roller.

REFERENCES:

[1] X. Kun, M. Tie and Y. Ying. 2015. Failure analysis on generator bearing of mw-class double-fed WTG in a farm, *Mechanical Research & Application*, 1(28), 138-139.

[2] W. Zhihui. 2011. *Analytical Research on Mechanical Properties of Aerial Rolling Bears*, MSc Thesis, Nanjing University of Aeronautics and Astronautics.

[3] H. Aijing, M. Wanli and T. Guiji. 2012. Rolling bearing fault feature extraction method based on ensemble empirical mode decomposition and kurtosis criterion, *Proc. CSEE*, 32(11), 106-111.

[4] Z. Jin, F. Zhipeng and Z. Fulei. 2011. Extraction of rolling bearing fault feature based on time-wavelet energy spectrum, *J. Mech. Engg.*, 47(17), 44-49. http://dx.doi.org/10.3901/JME.2011.17.044.

[5] J. Tan and Y. Shengfa. 2014. Rolling bearing faults diagnosis based on the improved wavelet neural network, *J. Huazhong Agricultural University*, 33(1), 131-136.

[6] M. Olave, X. Sagartzazu and J. Damian. 2010. Design of four contact-point slewing bearing with a new load distribution procedure to account for structural stiffness, *J. Mech. Design*, 132. http://dx.doi.org/10.1115/1.4000834.

[7] L. Kania, M. Krynke and E. Mazanek. 2012. A catalogue capacity of slewing bearings, *Mechanism and Machine Theory*, 58, 29-45. http://dx.doi.org/10.1016/j.mechmachtheory.2012.07.012.

[8] G. Kai, Y. Shihua and Z. Yuyan. 2013. Study on the calculation method of ball bearing mechanical characteristics considering elastohydrodynamic lubrication with spinning, *J. Mech. Engg*., 49(15), 62-67. http://dx.doi.org/10.3901/JME.2013.15.062.

[9] Z. Gang, N. Xiaoting and M. Qingtao. 2015. Research on design and mechanical properties of permanent magnetic bearings for vertical wind turbines, *Bearing*, 5, 1-7.

[10] L. Limin. 2013. Improvement of grinding fixture used for peach-shaped raceway model of three or four point angular contact ball bearing, *J. Harbin Bearing*, 34(2), 29-31.